RESEARCH ARTICLE

WILEY

Aberrant functional network connectivity in psychopathy from a large (*N* = 985) forensic sample

Flor A. Espinoza[1]* | **Victor M. Vergara[1]*** | **Daisy Reyes[1,2]** |
Nathaniel E. Anderson[1] | **Carla L. Harenski[1]** | **Jean Decety[7]** |
Srinivas Rachakonda[1] | **Eswar Damaraju[1]** | **Barnaly Rashid[1]** | **Robyn L. Miller[1]** |
Michael Koenigs[5] | **David S. Kosson[6]** | **Keith Harenski[1]** | **Kent A. Kiehl[1,4#]** |
Vince D. Calhoun[1,3#]

[1]The Mind Research Network, Albuquerque, New Mexico 87106

[2]Department of Mathematics and Statistics, University of New Mexico, Albuquerque, New Mexico 87131

[3]Department of Electrical and Computer Engineering, University of New Mexico, Albuquerque, New Mexico 87131

[4]Department of Psychology, University of New Mexico, Albuquerque, New Mexico 87131

[5]Department of Psychiatry, University of Wisconsin – Madison, Madison, Wisconsin

[6]Department of Psychology, Rosalind Franklin University, North Chicago, Illinois

[7]Departments of Psychology and Psychiatry and Behavioral Neuroscience, University of Chicago, Chicago, Illinois

Correspondence
Flor A. Espinoza, The Mind Research Network, Albuquerque, NM 87106, USA.
Email: fespinoza@mrn.org

Abstract

Psychopathy is a personality disorder characterized by antisocial behavior, lack of remorse and empathy, and impaired decision making. The disproportionate amount of crime committed by psychopaths has severe emotional and economic impacts on society. Here we examine the neural correlates associated with psychopathy to improve early assessment and perhaps inform treatments for this condition. Previous resting-state functional magnetic resonance imaging (fMRI) studies in psychopathy have primarily focused on regions of interest. This study examines whole-brain functional connectivity and its association to psychopathic traits. Psychopathy was hypothesized to be characterized by aberrant functional network connectivity (FNC) in several limbic/paralimbic networks. Group-independent component and regression analyses were applied to a data set of resting-state fMRI from 985 incarcerated adult males. We identified resting-state networks (RSNs), estimated FNC between RSNs, and tested their association to psychopathy factors and total summary scores (Factor 1, interpersonal/affective; Factor 2, lifestyle/antisocial). Factor 1 scores showed both increased and reduced functional connectivity between RSNs from seven brain domains (sensorimotor, cerebellar, visual, salience, default mode, executive control, and attentional). Consistent with hypotheses, RSNs from the paralimbic system—insula, anterior and posterior cingulate cortex, amygdala, orbital frontal cortex, and superior temporal gyrus—were related to Factor 1 scores. No significant FNC associations were found with Factor 2 and total PCL-R scores. In summary, results suggest that the affective and interpersonal symptoms of psychopathy (Factor 1) are associated with aberrant connectivity in multiple brain networks, including paralimbic regions.

---

*These authors contributed equally to the work.

#These senior authors contributed equally to the work.

1 | INTRODUCTION

Psychopathy is a personality disorder associated with lack of remorse, empathy, poor decision-making, and profound impulsivity (Hare, 2003). Psychopathy is known to affect ∼0.5%–1% of the general population, 20% of incarcerated offenders (Hare, 2003), and 10%–15% of substance abusers. Incarcerated individuals with psychopathy who are released from prison have higher recidivism rates than nonpsychopathic prisoners (Hemphill, Hare, & Wong, 1998).

Previous structural and functional MRI findings suggest that psychopathy is related to abnormalities in limbic and paralimbic regions (Anderson & Kiehl, 2012; Ermer, Cope, Nyalakanti, Calhoun, & Kiehl, 2012; Kiehl, 2006). However, only a few studies have examined whether there are abnormalities in the functional brain connectivity of individuals with psychopathy (Glenn, Han, Yang, Raine, & Schug, 2017; Juarez, Kiehl, & Calhoun, 2013; Kiehl, 2006; Motzkin, Newman, Kiehl, & Koenigs, 2011; Wolf et al., 2015; Yoder, Porges, & Decety, 2015). One study that used resting state magnetic resonance imaging (rs-fMRI) data and seed regions found a decrease in functional connectivity between the amygdala and the ventromedial prefrontal cortex (vmPFC) in individuals with psychopathy (Motzkin et al., 2011). The vmPFC is involved in decision-making and moral reasoning, and the amygdala is involved in emotions, survival instincts, and memory. Interactions between these areas are thought to be associated with emotional regulation, stimulus reinforcement, and aggression (Blair, 2008; Davidson, Putnam, & Larson, 2000; Delgado, Nearing, Ledoux, & Phelps, 2008; Milad, Rauch, Pitman, & Quirk, 2006). Wolf et al. (2015) found reduced integrity of the white matter connecting amygdala with vmPFC in psychopathy. Motzkin and colleagues also found significantly lower levels of functional connectivity between vmPFC and precuneus/posterior cingulate cortex and between vmPFC and amygdala in psychopathy (Motzkin et al., 2011). The precuneus and vmPFC are involved in self-processing, self-consciousness, and self-related representations (Buckner, Andrews-Hanna, & Schacter, 2008; Cavanna & Trimble, 2006). Other studies have reported psychopathy to be associated with dysfunctions of the orbitofrontal-limbic and prefrontal-temporo-parietal-limbic network areas (Del Casale et al., 2015), and have identified altered functional connectivity between three major cortical networks: the default mode network (DMN), frontal parietal network, and cingulo-opercular network (Philippi et al., 2015). The latter study used seed based functional connectivity and also found psychopathy scores to be associated with increases or decreases in small regions within distinct patterns of functional connectivity. A study by Poeppl et al. (2017) using activation likelihood estimation to meta-analyze brain activation changes in psychopathy across 28 fMRI studies demonstrated that psychopathy was consistently associated with abnormal brain activity of the bilateral prefrontal cortices and the right amygdala.

Emerging cognitive models of psychopathy have suggested that psychopathy-related emotional deficits are promoted by fundamental abnormalities in attention which can impair the integration of emotional information into higher order behavior (Newman, 1998). This idea has been recently expanded to incorporate network-based functional hypotheses suggesting poor network integration across the brain in psychopathy (Hamilton, Hiatt Racer, & Newman, 2015). A study based on independent component analysis (ICA), a data-driven approach, found significant associations between psychopathy scores and functional connectivity in three networks including the default mode network, frontoparietal network, and visual network in fMRI data collected during an auditory oddball task (Juarez et al., 2013). A review on brain imaging research on psychopathy by Umbach et al. (2015) empathizes the need of exploration of other brain regions and circuits besides the amygdala and prefrontal cortex that may give rise to different features of psychopathy.

In this study, we aimed to assess the effect psychopathy has on the whole brain functional connectivity at rest in a large number of incarcerated males. We hypothesized that by analyzing functional connectivity in the whole brain, we could uncover additional brain regions and networks associated with psychopathic traits not explored by seed or region of interest analysis. To investigate whole brain FNC and its association to psychopathy effects, we performed high model order group independent component analysis (Calhoun & Adali, 2012) on a large collection of resting state functional magnetic resonance imaging (rs-fMRI) data from 985 inmates to obtain resting state networks (RSNs) and their time-courses (TCs). Functional network connectivity was estimated as the pairwise correlations among the RSNs TCs. Our results show that psychopathy is associated with both increased and reduced functional connectivity in seven brain domains involving a total of 31 RSNs. Consistent with theory and research, the majority of the identified networks were associated with paralimbic system regions: insula, anterior and posterior cingulate, amygdala, orbital frontal cortex, and superior temporal gyrus (Kiehl, 2006). Additional networks outside the paralimbic system were also identified as well.

2 | METHODS

2.1 | Participants

Resting-state fMRI data were collected from 985 male prison inmates scanned with the Mind Research Network's 1.5 T mobile scanner. Inmates were located at one of eight prisons in New Mexico or Wisconsin where we have established research programs. Participants were between the ages of 18 and 63 (average age = 33.7 years, SD = 9 years). Participants' demographics and PCL-R scores are shown in Table 1.

TABLE 1 Participants demographics and PCL-R scores

	Mean	SD	Min.	25%	50%	75%	Max.
Age (years)	33.7	9.1	18	26	32	40	63
IQ	99	14.6	66	89	99	109	146
PCL-R score	22.2	6.5	3.2	18	22	26.7	40
PCL-R Factor 1	7.3	3.4	0	5	32	40	16
PCL-R Factor 2	12.7	3.5	2	11	12.7	15	20

2.2 | Psychopathy scores

Participants were assessed for psychopathy with the Hare Psychopathy Checklist-Revised (PCL-R) (Hare, 1991). The PCL-R is considered to be the most accepted measure for assessing psychopathy in forensic samples (Kiehl, 2006). The PCL-R consists of 20 items which are scored on a three-point scale, 0 (does not apply), 1 (applies somewhat), and 2 (definitely applies). It is based on participants' clinical interview and extensive file review conducted by trained Research Assistants. The resulting PCL-R scores range from 0 to 40. Factor analyses of the 20 PCL-R items have revealed two correlated factors. Factor 1 scores correspond to affective/interpersonal characteristics, whereas Factor 2 scores, correspond to impulsive, nomadic lifestyle and early and persistent antisocial behavior (Hare & Neumann, 2010; Harpur, Hare, & Hakstian, 1989). The PCL-R scores for this group ranged from 3.2 to 40 (mean 22.2, SD 6.5); 173 inmates were above the traditional clinical cutoff of 30 to be classified as psychopathic. PCL-R, Factor 1 and Factor 2 scores were treated as continuous variables and correlated to the rs-fMRI data. Table 1 contains a breakdown of the demographic characteristics for the participants in this study. The study was approved by the University of New Mexico's Human Research Institutional Review Board (IRB) and all participants provided written informed consent. Participants were paid at a rate commensurate with institution compensation for work assignments at their facility.

2.3 | Imaging parameters

Resting-state functional magnetic resonance images were collected on prison grounds using a mobile Siemens 1.5 T Avanto with advanced SQ gradients (max slew rate 200T/m/s, 346T/m/s vector summation, rise time 200 μs) equipped with a 12-element head coil. The EPI gradient-echo pulse sequence (TR 2000 ms,/TE = 39 ms, flip angle 90°, FOV 24 × 24 cm, 64 × 64 matrix, 3.4 × 3.4 mm in-plane resolution, 4 mm slice thickness, 1 mm gap, 30 slices) effectively covered the entire brain (150 mm) in 2.0 s. Head motion was minimized using padding and restraint. The participants were asked to lay still, look at the fixation cross and keep eyes open during the 5 min resting-state fMRI scanning. Compliance with instructions was monitored by eye tracking.

2.4 | EPI preprocessing

Data were preprocessed using statistical parametric mapping (Friston et al., 1994) (http://www.fil.ion.ucl.ac.uk/spm) including slice-timing correction, realignment, co-registration, and spatial normalization, and

then transformed to the Montreal Neurological Institute standard space at a resolution of a $3 \times 3 \times 3$ mm³. Despiking consisted of the orthogonalization with respect to spike regressors. Each spike is represented by an independent regressor valued at one at the spike time point and zero everywhere else. The DVARS method (Power, Barnes, Snyder, Schlaggar, & Petersen, 2012) was used to find spike regressors where the root mean square exceeded three standard deviations. Time-courses were also orthogonalized with respect to the following: (a) linear, quadratic, and cubic trends; (b) the six realignment parameters; (c) realignment parameters derivatives; and (d) spike regressors. A full width half maximum Gaussian kernel of 6 mm was then used for spatial smoothing. Framewise displacement (FD) was used to asses for motion quality control, as we did not have participants with FD above 3 mm for more than 10% of their total volume; no participants were removed due to severe motion.

2.5 | Independent component analysis

We applied group independent component analysis (GICA) on the preprocessed data using the GIFT toolbox (http://mialab.mrn.org/software/gift) (Calhoun, Adali, Pearlson, & Pekar, 2001). The rs-fMRI data was compressed using two stages of principal component analysis (PCA) (Rachakonda, Silva, Liu, & Calhoun, 2016). For the first data reduction, we retained $T = 100$ principal components (PCs). Based on previously published work (Allen et al., 2011), we chose to retain $C = 75$ independent components for group data reduction (Erhardt et al., 2011). Individual specific spatial maps and their time-courses were obtained using GICA. Out of the 75 ICs that were estimated, 55 components were identified as components of RSNs by evaluating the high to low frequency power in the spectra of components, and whether peak activations took place in gray matter (Allen et al., 2011; Meda et al., 2008; Robinson et al., 2009). The other 20 components were excluded as they appeared to be related to motion artifacts or the spatial maps including white matter, the ventricular system, or cerebral spinal fluid, or had irregular time course spectra power (Allen et al., 2011). The time-courses of the RSNs underwent despiking and band-pass by filtering with [0.01 0.15] Hz cutoffs. Before computing the FNC, the movement parameters (translation and rotation) and their derivatives were regressed out of the RSNs time-courses at the individual level to reduce variance associated with movement from the analyses (Vergara, Mayer, Damaraju, Hutchison, & Calhoun, 2017). Next, we calculated the FNC between the selected 55 RSNs as pairwise correlations between the RSNs time-courses for each individual.

2.6 | Statistical analyses

We performed regression analysis using four models (primary models 1 and 2, and two secondary models 3 and 4) for main effects of psychopathy to identify associations between individual FNC values and Psychopathy measures: PCL-R, Factor 1, and Factor 2. The models were corrected for "nuisance" covariates (age, IQ, rotation, and translation). For each participant, the translation and rotation parameters were computed as the mean of the sums of the absolute translation and
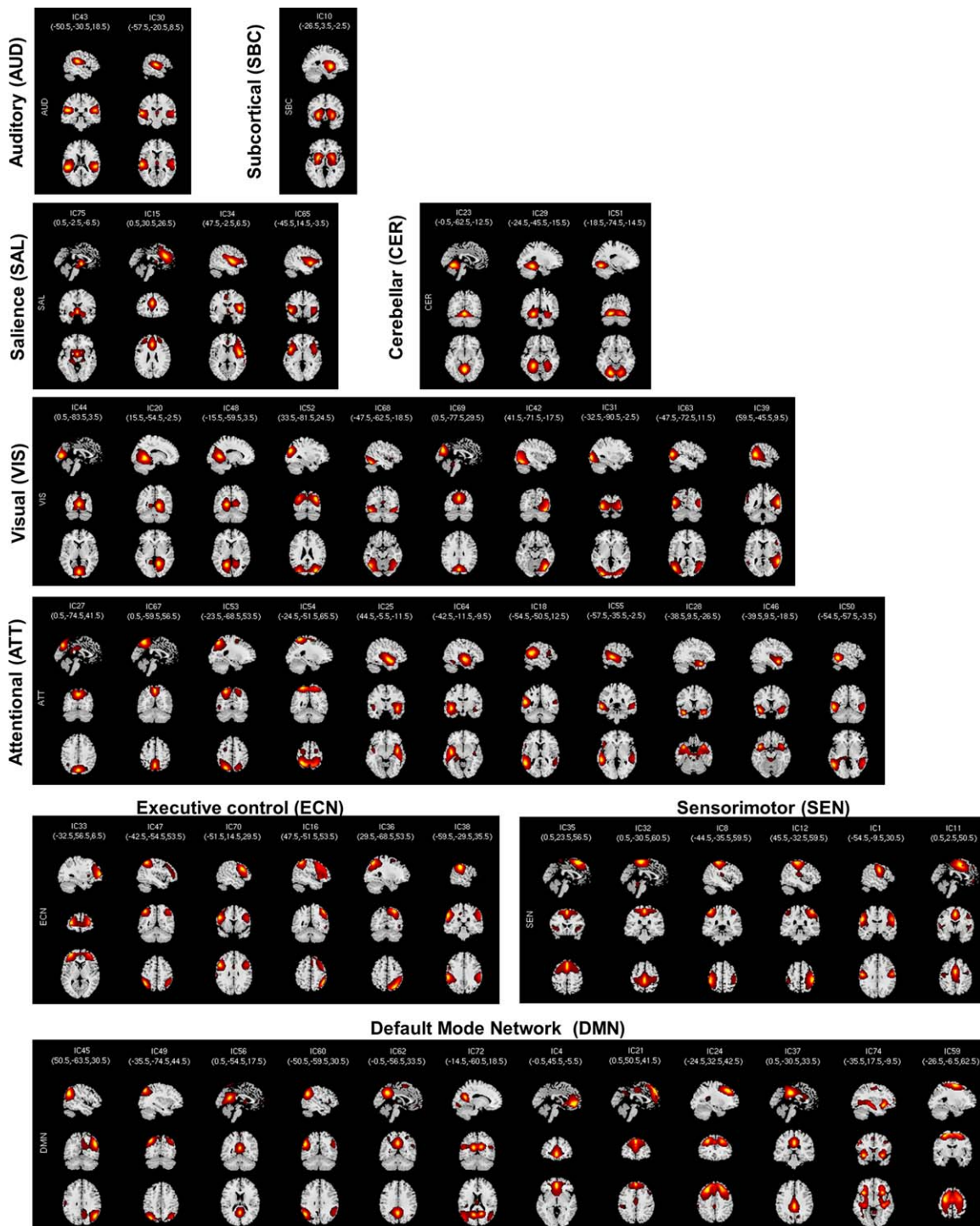
FIGURE 1 Spatial maps of the 55 independent components identified as RSNs. RSNs were separated into nine domains [subcortical (SBC), auditory (AUD), sensorimotor (SEN), cerebellar (CER), visual (VIS), salience (SAL), default mode network (DMN), executive control (ECN), and attentional (ATT)] based on their functional properties [Color figure can be viewed at wileyonlinelibrary.com]

rotation frame displacements. The main effects included in each of the four models were as follows: PCL-R total score (model 1); both Factor 1 and Factor 2 (model 2); just Factor 1 (model 3); and just Factor 2 (model 4). The significance of the univariate psychopathy results for each model was determined using a false discovery rate (FDR) (Genovese, Lazar, & Nichols, 2002) threshold at $p < .05$. Three participants were remove from the regression analysis for no having

PCL-R scores, their psychopathy scores were assessed with the PCL youth version.

3 | RESULTS

Figure 1 shows the spatial maps of the 55 selected RSNs; the functional connectivity between these RSNs are represented in Figure 2.
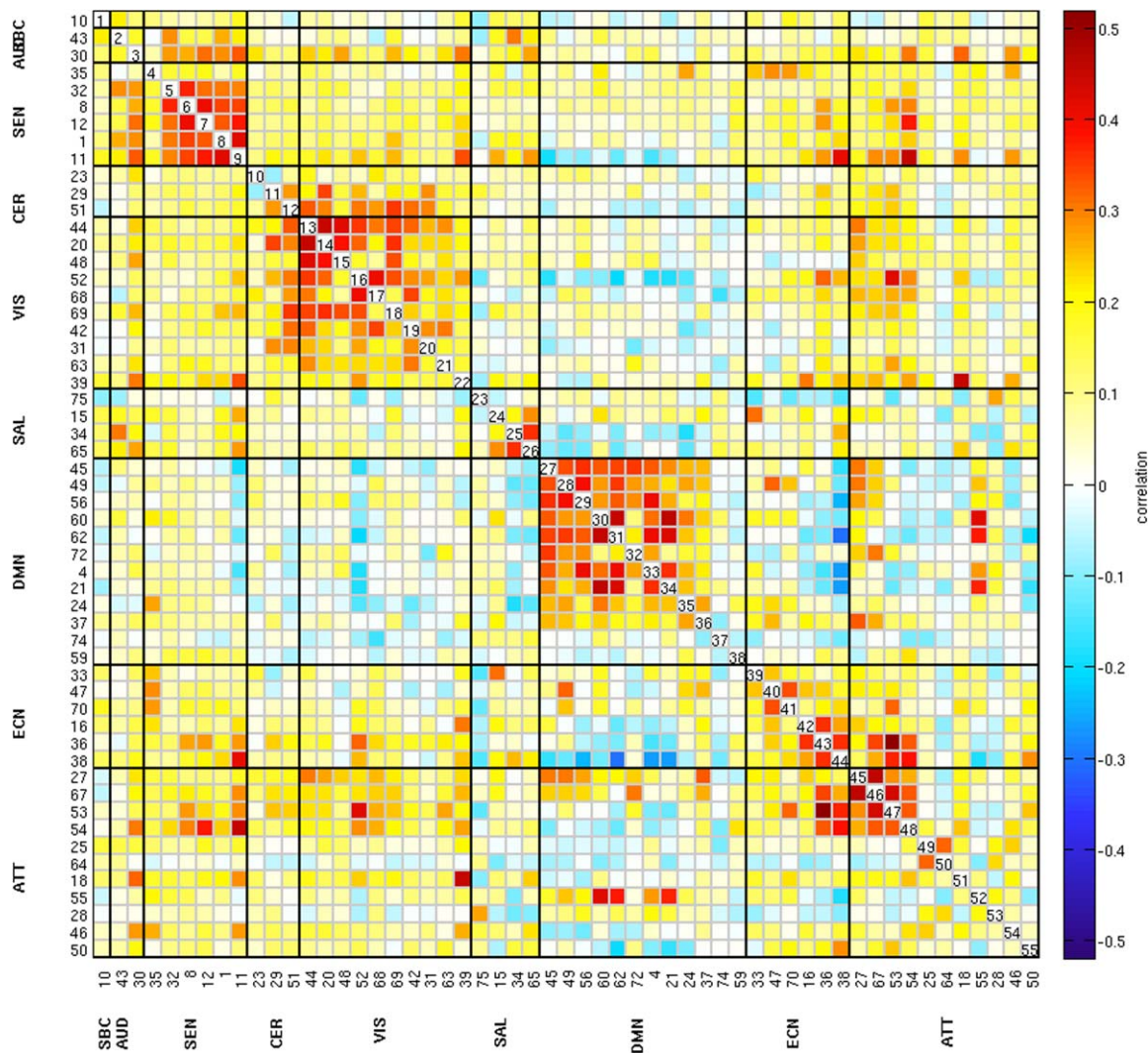
FIGURE 2 Functional network connectivity matrix of the 55 RSNs. Pairwise correlations between RSNs time-courses were Fisher z-transformed and averaged across subjects, and inverse z-transformed for display [Color figure can be viewed at wileyonlinelibrary.com]

The 55 RSNs listed in Table 2 were grouped into nine domains: sub-cortical (SBC), auditory (AUD), sensorimotor (SEN), cerebellar (CER), visual (VIS), salience (SAL), default mode network (DMN), executive control (ECN), and attentional (ATT) based on the automatic labeling tool in GIFT, neurosynth (neurosynth.org) and confirmed by visual inspection. From the FNC matrix shown in Figure 2, we can observe that the sensorimotor, visual and default mode network domains show mostly positive correlations among their RSNs. The default mode network shows mostly negative correlations with the subcortical, sensorimotor, cerebellar, visual, salience, executive control, and attentional RSNs. It also shows highly positive correlation with RSNs from the attentional domain.

Univariate test results (FDR corrected using a significance level of .05) for the first and fourth regression models revealed no significant associations between the FNC values and the PCL-R Total score or the Factor 2 scores. In the second regression model, we obtained significant associations between the FNC values and Factor 1 scores, but no significant associations survived FDR correction for Factor 2 scores. In the third regression model we obtained significant overlapping associations with regression model 2. The significant associations of Factor 1

scores with whole-brain functional connectivity from regression model 2 are shown in Figure 3. The analyses revealed 28 correlation pairs (31 RSNs from seven domains: SEN, CER, VIS, SAL, DMN, ECN, and ATT) showing significant positive (12 pairs) and negative (16 pairs) Factor 1 effects (RSNs, p and beta values are listed in Table 3). Positive Factor 1 effects imply that as Factor 1 scores increase, the functional connectivity between the RSNs: supplementary motor area [(SMA), IC35, SEN] and cerebellum Lobule VI [IC51, CER], superior occipital gyrus [IC52, VIS], cuneus [IC69, VIS], and superior occipital gyrus [IC42, VIS]; anterior cingulate cortex [(ACC), IC15, SAL] and left middle occipital gyrus [IC63, VIS], posterior cingulate cortex [(PCC), IC72, DMN], and middle frontal gyrus [IC70, ECN]; middle frontal gyrus [IC24, DMN] and cuneus [IC69, VIS]; right inferior occipital gyrus [IC42, VIS] and orbital frontal cortex [(OFC), IC33, ECN], and inferior parietal lobule [IC16, ECN]; inferior parietal lobule [IC38, ECN] and PCC [IC56, DMN]; cuneus [IC27, ATT] and cerebellum Lobule VI [IC51, CER] increases. On the other hand, negative Factor 1 effects imply that as Factor 1 scores increase, the functional connectivity between the RSNs: right lingual gyrus [IC20, VIS] and cerebellum Lobule VI [IC29, CER]; left

TABLE 2 Resting-state networks (RSNs) domain names, IC numbers, and MNI peak coordinates

RSNs and domain names		IC number MNI peak (x, y, z)
Subcortical (SBC)		
Putamen	10	(−26.5, 3.5, −2.5)
Auditory (AUD)		
Superior temporal gyrus (STG)	30	(−57.5, −20.5, 8.5)
Postcentral gyrus (PoCG)	43	(−50.5, −30.5, 18.5)
Sensorimotor (SEN)		
Supplementary motor area (SMA)	35	(0.5, 23.5, 56.5)
Paracentral lobule	32	(0.5, −30.5, 60.5)
Left postcentral gyrus (L-PoCG)	8	(−44.5, −35.5, 59.5)
Right postcentral gyrus (R-PoCG)	12	(45.5, −32.5, 59.5)
Precentral gyrus (PrCG)	1	(−54.5, −9.5, 30.5)
SMA	11	(0.5, 2.5, 50.5)
Cerebellar (CER)		
Cerebellum (CerB)	23	(−0.5, −62.5, −12.5)
Cerebellum lobule VI	29	(−24.5, −45.5, −15.5)
Bilateral cerebellum lobule VI	51	(−18.5, −74.5, −14.5)
Visual (VIS)		
Cuneus	44	(0.5, −83.5, 3.5)
Right lingual gyrus	20	(15.5, −54.5, −2.5)
Left lingual gyrus	48	(−15.5, −59.5, 3.5)
Superior occipital gyrus (SOccG)	52	(33.5, −81.5, 24.5)
Fusiform gyrus	68	(−47.5, −62.5, −18.5)
Cuneus	69	(0.5, −77.5, 29.5)
Right inferior occipital gyrus (R-InfOccG)	42	(41.5, −71.5, −17.5)
Middle occipital gyrus	31	(−32.5, −90.5, −2.5)
Left middle occipital gyrus	63	(−47.5, −72.5, 11.5)
Superior temporal gyrus (STG)	39	(59.5, −45.5, 9.5)
Salience (SAL)		
Amygdala	75	(0.5, −2.5, −6.5)
Anterior cingulate cortex (ACC)	15	(0.5, 30.5, 26.5)
Operculum/insula	34	(47.5, −2.5, 6.5)
Insula	65	(−45.5, 14.5, −3.5)
Default mode network (DMN)		
Right angular gyrus	45	(50.5, −63.5, 30.5)
Angular gyrus	49	(−35.5, −74.5, 44.5)
Posterior cingulate cortex (PCC)	56	(0.5, −54.5, 17.5)
Angular	60	(−50.5, −59.5, 30.5)
Precuneus/PCC	62	(−0.5, −56.5, 33.5)
Posterior cingulate cortex (PCC)	72	(−14.5, −60.5, 18.5)
Anterior cingulate cortex (ACC)	4	(−0.5, 45.5, −5.5)
Medial prefrontal cortex (Me-PFC)	21	(0.5, 50.5, 41.5)
Middle frontal gyrus (Mi-FG)	24	(−24.5, 32.5, 42.5)
Posterior cingulate gyrus (PCG)	37	(0.5, −30.5, 33.5)
Anterior cingulate cortex (ACC)	74	(−35.5, 17.5, −9.5)
Middle frontal gyrus	59	(−26.5, −6.5, 62.5)
Executive control (ECN)		
Orbital frontal cortex (OFC)	33	(−32.5, 56.5, 6.5)
Inferior parietal lobule	47	(−42.5, −54.5, 53.5)
Middle frontal gyrus (Mi-FG)	70	(−51.5, 14.5, 29.5)
Inferior parietal lobule	16	(47.5, −51.5, 53.5)
Superior parietal lobule	36	(29.5, −68.5, 53.5)
Left inferior perietal lobule	38	(−59.5, −29.5, 35.5)

(Continues)

TABLE 2 (Continued)

RSNs and domain names		IC number MNI peak (x, y, z)
Attentional (ATT)		
Cuneus	27	(0.5, −74.5, 41.5)
Precuneus	67	(0.5, −59.5, 56.5)
Superior parietal lobule	53	(−23.5, −68.5, 53.5)
Superior parietal lobule	54	(−24.5, −51.5, 65.5)
Superior temporal gyrus (STG)	25	(44.5, −5.5, −11.5)
Superior temporal gyrus (STG)	64	(−42.5, −11.5, −9.5)
Left middle temporal gyrus	18	(−54.5, −50.5, 12.5)
Middle temporal gyrus (Mi-TG)	55	(−57.5, −35.5, −2.5)
Temporal pole/STG	28	(−38.5, 9.5, −26.5)
Temporal pole/STG	46	(−39.5, 9.5, −18.5)
Middle temporal gyrus (Mi-TG)	50	(−54.5, −57.5, −3.5)

lingual gyrus [IC48, VIS] and right lingual gyrus [IC20, VIS]; operculum/insula [IC34, SAL] and SMA [IC11, SEN] and PCC [IC37, DMN]; insula [IC65, SAL] and precentral gyrus [IC1, SEN] and SMA [IC11, SEN]; left angular gyrus [IC49, DMN] and right angular gyrus [IC45, DMN]; left angular [IC60, DMN] and PCC [IC56, DMN]; cuneus [IC27, ATT] and amygdala [IC75, SAL]; left superior temporal gyrus [IC64, ATT] and superior occipital gyrus [IC52, VIS]; middle temporal gyrus [IC50, ATT] and precentral gyrus [IC1, SEN], SMA [IC11, SEN], cuneus [IC44, VIS], superior occipital gyrus [IC52, VIS], fusiform gyrus [IC68, VIS] and cuneus [IC69, VIS] decreases. We also observed decrease within functional connectivity in the visual [left lingual gyrus and right lingual gyrus (IC48–IC20)] and in the default mode network [left angular gyrus and right angular gyrus (IC49–IC45), and left angular and PCC (IC60–IC56)] domains associated with Factor 1 scores. Overall, there were both positive and negative correlation pairs showing significant functional connectivity effects between default mode network and visual [middle frontal gyrus and cuneus (IC24–IC69)]; salience [ACC and PCC (IC15–IC72) and PCC and operculum/insula (IC37–IC34)]; and executive control [PCC and inferior parietal lobule (IC56–IC38)] domains associated with Factor 1 scores.

4 | DISCUSSION

One of the most prominent neurobiological models of psychopathy focuses on dysfunctions in amygdala and ventromedial prefrontal cortex (vmPFC) (Anderson & Kiehl, 2012; Blair, 2006; Korponay et al., 2017). Imaging studies have been providing evidence for amygdala and prefrontal deficits in psychopathy (Blair, 2008; Kiehl et al., 2001; Koenigs, 2012; Motzkin et al., 2011; Müller et al., 2003; Philippi et al., 2015; Umbach et al., 2015; Yoder et al., 2015). The amygdala is important for the processing of emotionally salient information including threatening emotions and fear (Davis & Whalen, 2001). However, reports of damage to several other brain regions such as the anterior cingulate cortex (ACC) and the orbital frontal cortex (OFC) (Hornak et al., 2003) can result in changes in behavior mimicking some psychopathic traits. Comprehensive reviews of neurobiological literature show that neural dysfunction in psychopathy involves extensive limbic brain networks. Based on this evidence, a paralimbic-centered model
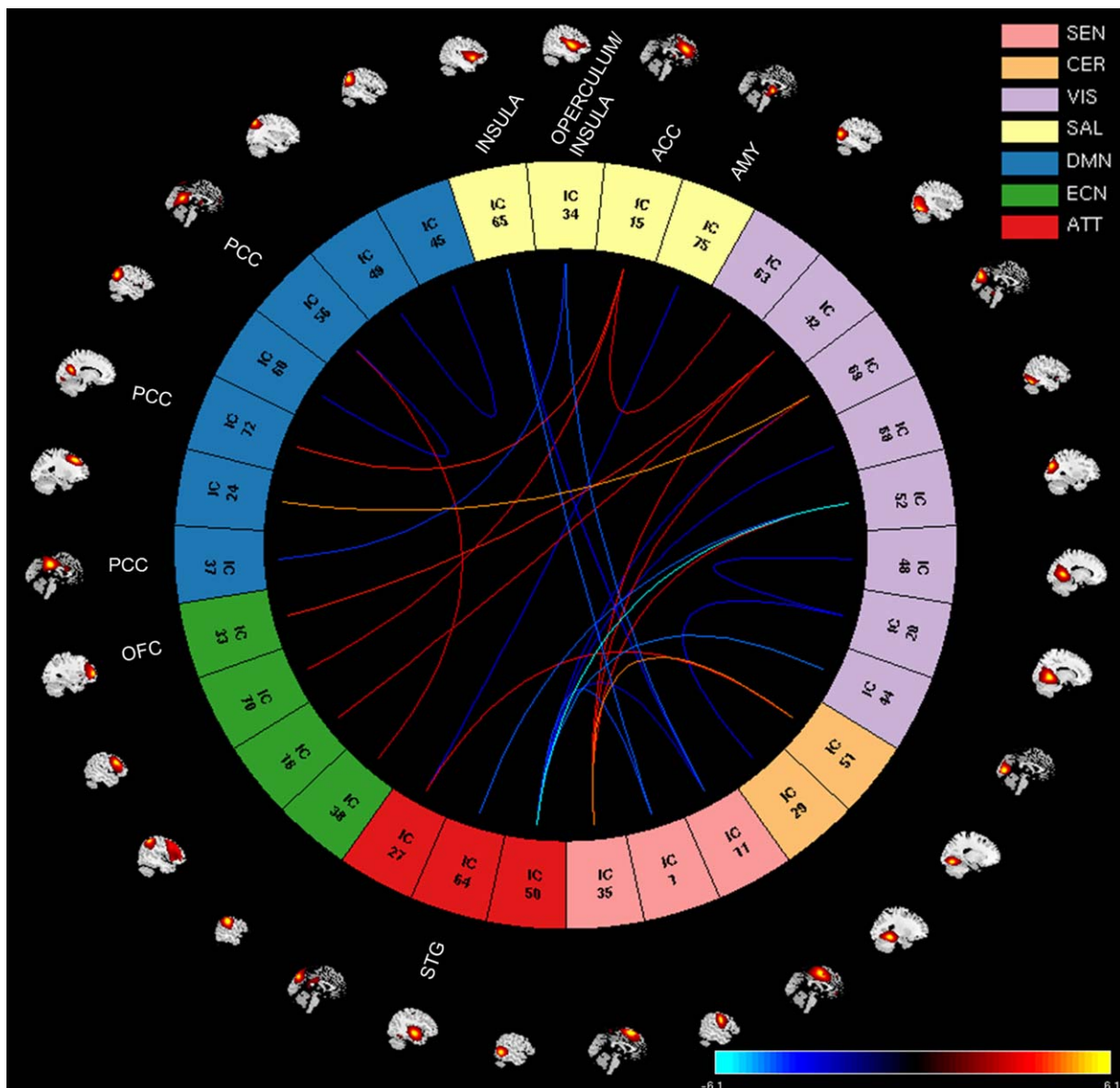
FIGURE 3 Factor 1 effects showing positive and negative associations with RSNs from seven brain domains: sensorimotor (SEN), cerebellar (CER), visual (VIS), salience (SAL), default mode network (DMN), executive control (ECN), and attentional (ATT). The significant associations between FNC values and Factor 1 scores are shown with connecting curves between networks displayed as −(beta)log10(p value), color bar ranging from −6.1 to 6.1. Red and orange colors correspond to positive correlations; and dark and light blue colors correspond to negative correlations. The RSNs from the paralimbic regions listed in the plot are orbital frontal cortex (OFC, IC33), insula (ICs: 65 and 34), anterior cingulate cortex (ACC, IC15), posterior cingulate cortex (PCC, ICs: 37, 72, and 56), amygdala (AMY, IC75), and superior temporal gyrus (STG, IC64). The rest of ICs are described in Table 2 [Color figure can be viewed at wileyonlinelibrary.com]

including the insula, amygdala and cingulate cortex has been proposed extending the amygdala-centered model to other brain areas (Anderson & Kiehl, 2012; Kiehl, 2006). This work is largely consistent with the paralimbic-centered model. Our results point to aberrant connectivity in several brain regions across the brain including those within the paralimbic system. The focus of several studies in psychopathy examines a set of brain areas widely considered to be important in processing salience information. Amygdala, insula and ACC have been identified as the three main components of this salience network (SAL) in charge of emotional attributes, and internal and external stimuli processing (interoception) that influences behavior (Hughes et al., 2015; Seeley et al.,

2007). Figure 4 displays the SAL as the center of the series of dysfunctions in our findings. Amygdala aberrations are very often associated with a diminished fear response (Lykken, 1957) which could affect moral behavior and decision making. However, instead of aberrant connectivity between amygdala and frontal brain areas that process risk, decision making, and control, our data points to a stronger reduction in connectivity between amygdala and cuneus (ICs 75 and 27; see Table 3). A closer look at the specific coordinates of the cuneus (IC27) using neurosynth (neurosynth.org) indicates that this component was linked to the default mode network (z-score 5.08 and 0.75 posterior probability), a RSN which is associated with self-referential processing. A recent

TABLE 3 Factor 1 effects, FDR-corrected results

RSNs pairs	ICs, domains	Beta	p value
Cerebellum lobule VI-SMA	51–35, CER-SEN	0.0088	2.37E-05
Right lingual gyrus, cerebellum lobule VI	20–29, VIS-CER	−0.0072	4.70E-04
Left lingual gyrus, right lingual gyrus	48–20, VIS-VIS	−0.0077	7.34E-04
Superior occipital gyrus, SMA	52–35, VIS-SEN	0.0076	4.05E-04
Cuneus, SMA	69–35, VIS-SEN	0.0072	6.34E-04
Right inferior occipital gyrus—SMA	42–35, VIS-SEN	0.0069	5.22E-04
ACC—left middle occipital gyrus	15–63, SAL-VIS	0.0073	6.51E-04
Operculum/insula—SMA	34–11, SAL-SEN	−0.0084	5.26E-05
Insula—precentral gyrus	65–1, SAL-SEN	−0.0082	5.70E-05
Insula—SMA	65–11, SAL-SEN	−0.0075	3.35E-04
Left angular gyrus—right angular gyrus	49–45, DMN-DMN	−0.0073	7.72E-04
Left angular—PCC	60–56, DMN-DMN	−0.0072	8.74E-04
PCC—ACC	72–15, DMN-SAL	0.0077	1.52E-04
Middle frontal gyrus—cuneus	24–69, DMN-VIS	0.0087	1.59E-05
PCC—operculum/insula	37–34, DMN-SAL	−0.0074	1.47E-04
Orbital frontal cortex—R-InfOccG	33–42, ECN-VIS	0.0080	1.07E-04
Middle frontal gyrus—ACC	70–15, ECN-SAL	0.0080	4.06E-04
Inferior parietal lobule—R-InfOccG	16–42, ECN-VIS	0.0079	2.15E-04
Inferior parietal lobule—PCC	38–56, ECN-DMN	0.0074	6.77E-04
Cuneus—cerebellum Lobule VI	27–51, ATT-CER	0.0082	2.47E-04
Cuneus—amygdala	27–75, ATT-SAL	−0.0064	7.96E-04
Left superior temporal gyrus—SOccG	64–52, ATT-VIS	−0.0082	4.15E-05
(Mi-TG)—precentral gyrus	50–1, ATT-SEN	−0.0084	7.16E-05
(Mi-TG)—SMA	50–11, ATT-SEN	−0.0072	8.98E-04
(Mi-TG)—cuneus	50–44, ATT-VIS	−0.0082	3.73E-05
(Mi-TG)—superior occipital gyrus	50–52, ATT-VIS	−0.0107	7.82E-07
(Mi-TG)—fusiform gyrus	50–68, ATT-VIS	−0.0071	8.35E-04
(Mi-TG)—cuneus	50–69, ATT-VIS	−0.0072	6.89E-04

study by Anderson et al. demonstrated that PCL-R Factor 1 scores are associated with relatively reduced emotion-driven upregulation of activity in visual processing areas (mediated by amygdala function). The authors speculated that there may be a functional disconnection between amygdala and occipital regions that could interfere with this emotion/salience-driven upregulation (Anderson et al., 2017).

Aberrant functional connectivity in areas, including amygdala, insula, and areas of self-referential functions, such as anterior cingulate cortex and ventromedial prefrontal cortex, is thought to have a strong link to the lack of empathy and to the way psychopaths relate themselves to others (Blair, 2006; Decety & Cowell, 2014; Modinos, Ormel, & Aleman, 2009) . Self-referential dysfunction is further supported by the decrement in connectivity between insula, DMN, and sensorimotor areas. The insula is an important area of the brain involved in cognitive,

affective, and regulatory functions such as interoceptive awareness, empathic processes, emotional responses, and processing of internal and external stimuli (Menon, 2011). Reciprocal projections between the insula and somatosensory areas, and the cingulate gyrus, have been identified through histochemical and radiographic techniques (Flynn, 1999). Dysfunctions in these connections may be related to individual problems in feeling and empathy as the insula plays an important role in these behaviors (Singer, Critchley, & Preuschoff, 2009). These results are also consistent with cognitive theories of psychopathy that have suggested poor network integration as the source of fundamental psychopathic deficits (Hamilton et al., 2015; Newman, 1998). Hamilton's study suggests impairments across salience and DMN networks, which may be etiologically fundamental to the apparent deficits in adequate processing of emotionally salient information in the environment.
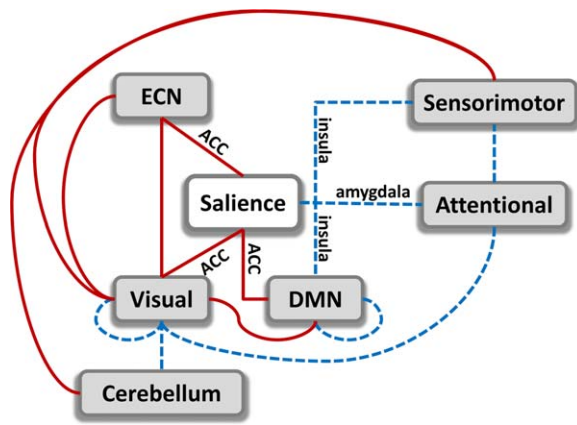
FIGURE 4 Summary of dysfunctional connections among networks from six domains: executive control (ECN), salience, visual, default mode network (DMN), sensorimotor, and attentional. Increased connectivity is indicated in red solid lines and decreased connectivity in blue dashed lines. The main focus is the salience network composed of anterior cingulate cortex (ACC), insula, and amygdala. In the salience network, all redlines belong to ACC, while blue lines belong to amygdala and insula [Color figure can be viewed at wileyonlinelibrary.com]

Similarly, these studies suggest Factor 1 of PCL-R is more closely associated with these deficits than Factor 2.

Our results are also in line with the paralimbic system dysfunction model of psychopathy introduced by (Kiehl, 2006) that includes the ACC, PCC, OFC, insula, amygdala, parahippocampal gyrus, and anterior superior temporal gyrus as neural regions implicated in psychopathy. Interestingly, in this study, the ACC connectivity goes in the opposite direction (increased connectivity between ACC and left middle occipital gyrus, posterior cingulate cortex, and middle frontal gyrus, Table 3) than the insula and amygdala (decreased connectivity between insula and precentral gyrus, supplementary motor area, and between amygdala and cuneus). A gross interpretation of this effect is a compensation mechanism of increments and decrements in connectivity among different areas of ECN, SAL, and DMN (Menon, 2011; Sridharan, Levitin, & Menon, 2008). A closer look at evidence from previous studies could clarify the consequences of this compensation. The ACC is a region that has been classically linked to reward and decision making (Kolling, Behrens, Wittmann, & Rushworth, 2016; Ullsperger, Fischer, Nigbur, & Endrass, 2014), but other recent views suggest that ACC is involved in social behavior as an area that tracks the motivation of others (Apps, Rushworth, & Chang, 2016). Understanding others motivation might be linked to the manipulative trait observed in psychopaths. Manipulation and impairment in recognizing emotional facial expressions could be linked to the set of dysfunctions between ECN, Visual and salient ACC networks portrayed in Figure 4 in relation to the way psychopaths perceive other people. However, dysfunction involving the DMN points to introspective processing and it is necessary to analyze how psychopaths see themselves. In this respect, a study explored the brain of psychopaths while they viewed bodily injuries with the tasks of imagine-self or imagine-others perspectives (Decety, Chen, Harenski, & Kiehl, 2013). The results indicate that psychopaths exhibit a normal connectivity pattern when adopting a self-referential perspective, but a dysfunctional connectivity while imagining the perspective of others. Furthermore, the dysfunctional pattern observed with respect to the insula is consistent with the anomalies observed in our study. In our data, an imagine-self perspective was not encouraged, and it is plausible that subjects were not engaged in this mode since they were instructed to be free of any specific task. It could be argued that the lack of an imagine-self perspective might have triggered the dysfunctional connectivity state. An imagine others perspective was not necessary to observe the anomalous connectivity of the salience network. In summary, the connectivity dysfunctions in Figure 4 points to a compensation mechanism resulting in an enhanced ability of tracking the motivation of others that facilitates manipulative behavior, due to a hyperconnected ACC, while reduced empathy, thanks to a hypoconnected amygdala and insula. Overall our findings are in alignment with the triple network model of psychopathology (Menon, 2011) which states that aberrant organization and functioning of the ECN, SAL, and DMN are prominent features of several major psychiatric and neurological disorders. In addition, the ECN, SAL, and DMN networks are part of the six types of circuit dysfunction that contribute to the variability in depression and anxiety (Williams, 2017). Further investigation of connectivity among these networks can provide better understanding of brain disruptions in psychopathy and other psychiatric disorders such as schizophrenia, depression, autism, and anxiety disorders.

4.1 | Study limitations

There are a number of limitations to consider in this study. First, because this was a resting-state fMRI study, it is hard to attribute the changes to a specific functional domain. Studies which combine extended rest and task data are needed to address this point (Cetin et al., 2014). In addition, because this study was limited to a forensic population, it is difficult to determine whether the results would be the same for individuals who score high on psychopathy but were not incarcerated. Finally, this study makes the assumption that connectivity among networks is consistent throughout the 5-min scan duration. Future work should also focus on time-varying or dynamic connectivity which may provide additional information when considering time-dependent FNC (Calhoun, Miller, Pearlson, & Adalı, 2014).

5 | CONCLUSION

This study adds to the current literature by unrestrictedly examining functional connectivity in the whole brain and analyzing its association to psychopathy traits. Using of the largest forensic neuroimaging sample to date (N = 985 inmates), group-independent component and statistical analysis, we showed that psychopathy (Factor 1 scores) is associated with both increased and decreased functional connectivity among 31 out of 55 identified RSNs from seven brain domains (sensorimotor, cerebellar, visual, salience, default mode network, executive control, and attentional). Consistent with theory and research, our results are in agreement with many studies which found that anomalies in paralimbic regions (insula, anterior and posterior cingulate cortex, amygdala, superior temporal gyrus, and orbital frontal cortex) are

closely related to psychopathy, and emerging research implicating poor integration between functional networks in psychopathy. Our results did not reveal significant relationships for FNC with Factor 2 (lifestyle/antisocial) and total PCL-R scores, suggesting that the abnormal connectivity findings in resting-state brain connectivity may be more specific to Factor 1 (interpersonal and affective traits of psychopathy) than is indicated by most prior theories. Developmental studies are needed to see whether the alterations in functional connectivity related to Factor 1 scores are early-emerging. To the best of our knowledge, this represents the largest study to date focused on psychopathy-related intrinsic network interactions.

AUTHOR DISCLOSURE STATEMENT

No competing financial interest exists.

ORCID

Flor A. Espinoza [iD] http://orcid.org/0000-0001-8465-4543
Victor M. Vergara [iD] http://orcid.org/0000-0001-9404-0924
Carla L. Harenski [iD] http://orcid.org/0000-0003-4382-6921
Barnaly Rashid [iD] http://orcid.org/0000-0002-3602-5109

REFERENCES

Allen, E. A., Erhardt, E. B., Damaraju, E., Gruner, W., Segall, J. M., Silva, R. F., . . . Calhoun, V. D. (2011). A baseline for the multivariate comparison of resting-state networks. *Frontiers in Systems Neuroscience*, *5*, 2.

Anderson, N. E., & Kiehl, K. A. (2012). The psychopath magnetized: Insights from brain imaging. *Trends in Cognitive Sciences*, *16*(1), 52–60.

Anderson, N. E., Steele, V. R., Maurer, J. M., Rao, V., Koenigs, M. R., Decety, J., . . . Kiehl, K. A. (2017). Differentiating emotional processing and attention in psychopathy with functional neuroimaging. *Cognitive, Affective, & Behavioral Neuroscience*, *17*, 491–515.

Apps, M. A., Rushworth, M. F., & Chang, S. W. (2016). The anterior cingulate gyrus and social cognition: Tracking the motivation of others. *Neuron*, *90*(4), 692–707.

Blair, R. J. (2006). The emergence of psychopathy: Implications for the neuropsychological approach to developmental disorders. *Cognition*, *101*(2), 414–442.

Blair, R. J. (2008). The amygdala and ventromedial prefrontal cortex: Functional contributions and dysfunction in psychopathy. *Philosophical Transactions of the Royal Society B: Biological Sciences*, *363*(1503), 2557–2565.

Buckner, R. L., Andrews-Hanna, J. R., & Schacter, D. L. (2008). The brain's default network: Anatomy, function, and relevance to disease. *Annals of the New York Academy of Sciences*, *1124*, 1–38.

Calhoun, V. D., & Adali, T. (2012). Multisubject independent component analysis of fMRI: A decade of intrinsic networks, default mode, and neurodiagnostic discovery. *IEEE Reviews in Biomedical Engineering*, *5*, 60–73.

Calhoun, V. D., Adali, T., Pearlson, G. D., & Pekar, J. J. (2001). A method for making group inferences from functional MRI data using independent component analysis. *Human Brain Mapping*, *14*(3), 140–151.

Calhoun, V. D., Miller, R., Pearlson, G., & Adalı, T. (2014). The chronnectome: Time-varying connectivity networks as the next frontier in fMRI data discovery. *Neuron*, *84*(2), 262–274.

Cavanna, A. E., & Trimble, M. R. (2006). The precuneus: A review of its functional anatomy and behavioural correlates. *Brain: A Journal of Neurology*, *129*(Pt 3), 564–583.

Cetin, M. S., Christensen, F., Abbott, C. C., Stephen, J. M., Mayer, A. R., Canive, J. M., . . . Calhoun, V. D. (2014). Thalamus and posterior temporal lobe show greater inter-network connectivity at rest and across sensory paradigms in schizophrenia. *NeuroImage*, *97*, 117–126.

Davidson, R. J., Putnam, K. M., & Larson, C. L. (2000). Dysfunction in the neural circuitry of emotion regulation–a possible prelude to violence. *Science*, *289*(5479), 591–594.

Davis, M., & Whalen, P. J. (2001). The amygdala: Vigilance and emotion. *Molecular Psychiatry*, *6*(1), 13–34.

Decety, J., Chen, C., Harenski, C., & Kiehl, K. A. (2013). An fMRI study of affective perspective taking in individuals with psychopathy: Imagining another in pain does not evoke empathy. *Frontiers in Human Neuroscience*, *7*, 489.

Decety, J., & Cowell, J. M. (2014). The complex relation between morality and empathy. *Trends in Cognitive Sciences*, *18*(7), 337–339.

Del Casale, A., Kotzalidis, G. D., Rapinesi, C., Di Pietro, S., Alessi, M. C., Di Cesare, G., . . . Ferracuti, S. (2015). Functional neuroimaging in psychopathy. *Neuropsychobiology*, *72*(2), 97–117.

Delgado, M. R., Nearing, K. I., Ledoux, J. E., & Phelps, E. A. (2008). Neural circuitry underlying the regulation of conditioned fear and its relation to extinction. *Neuron*, *59*(5), 829–838.

Erhardt, E. B., Rachakonda, S., Bedrick, E. J., Allen, E. A., Adali, T., & Calhoun, V. D. (2011). Comparison of multi-subject ICA methods for analysis of fMRI data. *Human Brain Mapping*, *32*(12), 2075–2095.

Ermer, E., Cope, L. M., Nyalakanti, P. K., Calhoun, V. D., & Kiehl, K. A. (2012). Aberrant paralimbic gray matter in criminal psychopathy. *Journal of Abnormal Psychology*, *121*(3), 649–658.

Flynn, F. G. (1999). Anatomy of the insula functional and clinical correlates. *Aphasiology*, *13*(1), 55–78.

Friston, K. J., Holmes, A. P., Worsley, K. J., Poline, J. P., Frith, C. D., & Frackowiak, R. S. J. (1994). Statistical parametric maps in functional imaging: A general linear approach. *Human Brain Mapping*, *2*(4), 189–210.

Genovese, C. R., Lazar, N. A., & Nichols, T. (2002). Thresholding of statistical maps in functional neuroimaging using the false discovery rate. *NeuroImage*, *15*(4), 870–878.

Glenn, A. L., Han, H., Yang, Y., Raine, A., & Schug, R. A. (2017). Associations between psychopathic traits and brain activity during instructed false responding. *Psychiatry Research*, *266*, 123–137.

Hamilton, R. K., Hiatt Racer, K., & Newman, J. P. (2015). Impaired integration in psychopathy: A unified theory of psychopathic dysfunction. *Psychology Review*, *122*(4), 770–791.

Hare, R. D. (1991). *Manual for the hare psychopathy checklist-revised*. Toronto, ON: Multi-Health Systems.

Hare, R. D. (2003). *Manual for the hare psychopathy checklist-revised*. Toronto, ON: Multi-Health Systems.

Hare, R. D., & Neumann, C. S. (2010). Psychopathy: Assessment and forensic implications. *Responsibility and Psychopathy: Interfacing Law, Psychiatry and Philosophy*, 93–123.

Harpur, T. J., Hare, R. D., & Hakstian, A. R. (1989). Two-factor conceptualization of psychopathy: Construct validity and assessment implications. *Psychological Assessment: A Journal of Consulting and Clinical Psychology*, 1(1), 6.

Hemphill, J. F., Hare, R. D., & Wong, S. (1998). Psychopathy and recidivism: A review. *Legal and Criminological Psychology*, 3(1), 139–170.

Hornak, J., Bramham, J., Rolls, E. T., Morris, R. G., O'Doherty, J., Bullock, P. R., & Polkey, C. E. (2003). Changes in emotion after circumscribed surgical lesions of the orbitofrontal and cingulate cortices. *Brain: A Journal of Neurology*, 126(7), 1691–1712.

Hughes, M. A., Dolan, M. C., & Stout, J. C. (2015). Decision-making in psychopathy. *Psychiatry, Psychology and Law*, 23(4), 521–537.

Juarez, M., Kiehl, K. A., & Calhoun, V. D. (2013). Intrinsic limbic and paralimbic networks are associated with criminal psychopathy. *Human Brain Mapping*, 34(8), 1921–1930.

Kiehl, K. A. (2006). A cognitive neuroscience perspective on psychopathy: Evidence for paralimbic system dysfunction. *Psychiatry Research*, 142(2–3), 107–128.

Kiehl, K. A., Smith, A. M., Hare, R. D., Mendrek, A., Forster, B. B., Brink, J., & Liddle, P. F. (2001). Limbic abnormalities in affective processing by criminal psychopaths as revealed by functional magnetic resonance imaging. *Biological Psychiatry*, 50(9), 677–684.

Koenigs, M. (2012). The role of prefrontal cortex in psychopathy. *Reviews in the Neurosciences*, 23, 253–262.

Kolling, N., Behrens, T., Wittmann, M. K., & Rushworth, M. (2016). Multiple signals in anterior cingulate cortex. *Current Opinion in Neurobiology*, 37, 36–43.

Korponay, C., Pujara, M., Deming, P., Philippi, C., Decety, J., Kosson, D. S., ... Koenigs, M. (2017). Impulsive-antisocial psychopathic traits linked to increased volume and functional connectivity within prefrontal cortex. *Social Cognitive and Affective Neuroscience*, 2(2), 149.

Lykken, D. T. (1957). A study of anxiety in the sociopathic personality. *Journal of Abnormal Psychology*, 55(1), 6–10.

Meda, S. A., Giuliani, N. R., Calhoun, V. D., Jagannathan, K., Schretlen, D. J., Pulver, A., ... Pearlson, G. D. (2008). A large scale (N=400) investigation of gray matter differences in schizophrenia using optimized voxel-based morphometry. *Schizophrenia Research*, 101(1–3), 95–105.

Menon, V. (2011). Large-scale brain networks and psychopathology: A unifying triple network model. *Trends in Cognitive Sciences*, 15(10), 483–506.

Milad, M. R., Rauch, S. L., Pitman, R. K., & Quirk, G. J. (2006). Fear extinction in rats: Implications for human brain imaging and anxiety disorders. *Biological Psychology*, 73(1), 61–71.

Modinos, G., Ormel, J., & Aleman, A. (2009). Activation of anterior insula during self-reflection. *PLoS One*, 4(2), e4618.

Motzkin, J. C., Newman, J. P., Kiehl, K. A., & Koenigs, M. (2011). Reduced prefrontal connectivity in psychopathy. *Journal of Neuroscience*, 31(48), 17348–17357.

Müller, J. L., Sommer, M., Wagner, V., Lange, K., Taschler, H., Röder, C. H., ... Hajak, G. (2003). Abnormalities in emotion processing within cortical and subcortical regions in criminal psychopaths. *Biological Psychiatry*, 54(2), 152–162.

Newman, J. P. (1998). Psychopathic behavior: An information processing perspective. In D. J. Cooke, R. D. Hare, & A. Forth (Eds.), *Psychopathy: Theory, research and implications for society* (Vol. 88, pp. 81–104). Dordrecht, The Netherlands: Kluwer Academic Publishers.

Philippi, C. L., Pujara, M. S., Motzkin, J. C., Newman, J., Kiehl, K. A., & Koenigs, M. (2015). Altered resting-state functional connectivity in cortical networks in psychopathy. *Journal of Neuroscience*, 35(15), 6068–6078.

Poeppl, T., Donges, M., Rupprecht, R., Fox, P., Laird, A., Bzdok, D., ... Eickhoff, S. (2017). Meta-analysis of aberrant brain activity in psychopathy. *European Psychiatry*, 41, S349.

Power, J. D., Barnes, K. A., Snyder, A. Z., Schlaggar, B. L., & Petersen, S. E. (2012). Spurious but systematic correlations in functional connectivity MRI networks arise from subject motion. *NeuroImage*, 59(3), 2142–2154.

Rachakonda, S., Silva, R. F., Liu, J., & Calhoun, V. D. (2016). Memory efficient PCA methods for large group ICA. *Frontiers in Neuroscience*, 10,

Robinson, S., Basso, G., Soldati, N., Sailer, U., Jovicich, J., Bruzzone, L., ... Moser, E. (2009). A resting state network in the motor control circuit of the basal ganglia. *BMC Neuroscience*, 10(1), 137.

Seeley, W. W., Menon, V., Schatzberg, A. F., Keller, J., Glover, G. H., Kenna, H., ... Greicius, M. D. (2007). Dissociable intrinsic connectivity networks for salience processing and executive control. *Journal of Neuroscience*, 27(9), 2349–2356.

Singer, T., Critchley, H. D., & Preuschoff, K. (2009). A common role of insula in feelings, empathy and uncertainty. *Trends in Cognitive Sciences*, 13(8), 334–340.

Sridharan, D., Levitin, D. J., & Menon, V. (2008). A critical role for the right fronto-insular cortex in switching between central-executive and default-mode networks. *Proceedings of the National Academy of Sciences of the United States of America*, 105(34), 12569–12574.

Ullsperger, M., Fischer, A. G., Nigbur, R., & Endrass, T. (2014). Neural mechanisms and temporal dynamics of performance monitoring. *Trends in Cognitive Sciences*, 18(5), 259–267.

Umbach, R., Berryessa, C. M., & Raine, A. (2015). Brain imaging research on psychopathy: Implications for punishment, prediction, and treatment in youth and adults. *Journal of Criminal Justice*, 43(4), 295–306.

Vergara, V. M., Mayer, A. R., Damaraju, E., Hutchison, K., & Calhoun, V. D. (2017). The effect of preprocessing pipelines in subject classification and detection of abnormal resting state functional network connectivity using group ICA. *NeuroImage*, 145, 365–376.

Williams, L. M. (2017). Defining biotypes for depression and anxiety based on large-scale circuit dysfunction: A theoretical review of the evidence and future directions for clinical translation. *Depression and Anxiety*, 34(1), 9–24.

Wolf, R. C., Pujara, M. S., Motzkin, J. C., Newman, J. P., Kiehl, K. A., Decety, J., ... Koenigs, M. (2015). Interpersonal traits of psychopathy linked to reduced integrity of the uncinate fasciculus. *Human Brain Mapping*, 36(10), 4202–4209.

Yoder, K. J., Porges, E. C., & Decety, J. (2015). Amygdala subnuclei connectivity in response to violence reveals unique influences of individual differences in psychopathic traits in a nonforensic sample. *Human Brain Mapping*, 36(4), 1417–1428.